HHS Public Access

Author manuscript

J Neurochem. Author manuscript; available in PMC 2019 May 01.

Published in final edited form as:

J Neurochem. 2018 May ; 145(3): 232–244. doi:10.1111/jnc.14279.

Increased acetylcholine and glutamate efflux in the prefrontal cortex following intranasal orexin-A (hypocretin-1)

Coleman B. Calva, **Habiba Fayyaz**, and **Jim R. Fadel**[1]

Department of Pharmacology, Physiology and Neuroscience, University of South Carolina School of Medicine, Columbia, South Carolina, 29208 USA

Abstract

Orexin/hypocretin neurons of the lateral hypothalamus and perifornical area (LH/PFA) are integrators of physiological function. Previous work from our lab and others has shown the importance of orexin transmission in cognition. Age-related reductions in markers of orexin function further suggest that this neuropeptide may be a useful target for the treatment of age-related cognitive dysfunction. Intranasal administration of orexin-A (OxA) has shown promise as a therapeutic option for cognitive dysfunction. However, the neurochemical mechanisms of intranasal OxA administration are not fully understood. Here, we use immunohistochemistry and *in vivo* microdialysis to define the effects of acute intranasal OxA administration on: 1) activation of neuronal populations in the cortex, basal forebrain, and brainstem and 2) acetylcholine (ACh) and glutamate efflux in the prefrontal cortex (PFC) of Fischer 344/Brown Norway F1 (FBN F1) rats. Acute intranasal administration of OxA significantly increased c-Fos expression, a marker for neuronal activation, in the PFC and in subpopulations of basal forebrain cholinergic neurons. Subsequently, we investigated the effects of acute intranasal OxA on neurotransmitter efflux in the PFC and found that intranasal OxA significantly increased both ACh and glutamate efflux in this region. These findings were independent from any changes in c-Fos expression in orexin neurons, suggesting that these effects are not resultant from direct activation of orexin neurons. In total, these data indicate that intranasal OxA may enhance cognition through activation of distinct neuronal populations in the cortex and basal forebrain and through increased neurotransmission of ACh and glutamate in the PFC.

Graphical abstract

[1]Corresponding author: Jim Fadel, Dept. of Pharmacology, Physiology and Neuroscience, University of South Carolina School of Medicine, 6439 Garners Ferry Road, Columbia, SC 29208, Tel: (803) 216-3505, Fax: (803) 216-3538, jim.fadel@uscmed.sc.edu. DR. JIM FADEL (Orcid ID : 0000-0002-5221-1702)

All authors declare no financial conflicts of interest.

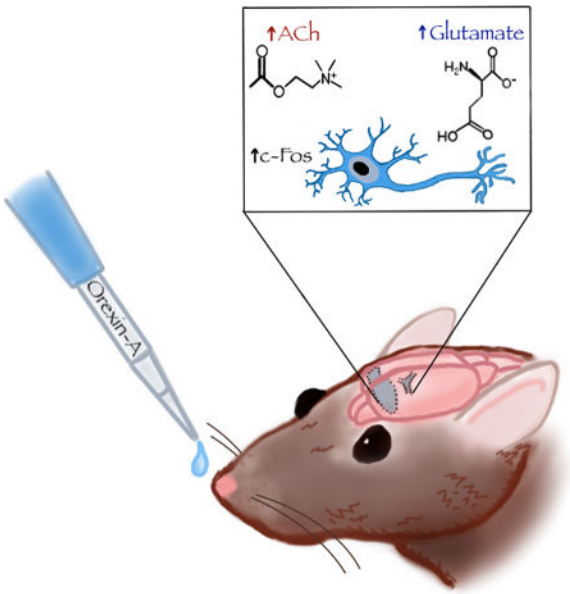

Orexins are peptides produced in the hypothalamus that influence arousal, feeding and cognition. A small body of literature suggests the utility of intranasal orexin administration for targeting the brain, but the brain regions and neurotransmitters that mediate these effects are not yet clear. Following intranasal orexin-A administration in young rats, we used immunohistochemistry and in-*vivo* microdialysis to investigate neuronal activation (c-Fos expression) and changes in acetylcholine and glutamate efflux in the prefrontal cortex. We show that intranasal orexin-A increases c-Fos expression in multiple cortical and basal forebrain regions and also significantly increases prefrontal cortical efflux of acetylcholine and glutamate.

Keywords

orexin; hypocretin; acetylcholine; intranasal; microdialysis; cognition

Introduction

The hypothalamus is the primary central nervous system locus for coordinating endocrine, autonomic and behavioral responses to peripheral cues indicative of homeostatic status. Although the mammalian hypothalamus contains a divergent array of nuclei and neural signaling molecules, the orexin (hypocretin) system plays a particularly prominent role in physiological regulation. The orexin system originates with neurons largely restricted to a posterior hypothalamic level that includes the lateral hypothalamus, perifornical area and parts of the dorsomedial nucleus, but gives rise to widespread projections that regulate limbic, cortical and brain stem circuits (Peyron et al. 1998). This diverse array of projections is consistent with the description of orexins as ‘physiological integrators’ (Li et al. 2014), but also suggests the potential to modulate cognition. For example, orexin-A (OxA) administration modulates glutamatergic thalamocortical synapses and facilitates attention (Lambe et al. 2005; Huang et al. 2006; Song et al. 2006). Administration of OxA has also been shown to facilitate attentional processing through activation of basal forebrain

cholinergic neurons, which in turn alter cortical acetylcholine release (Fadel et al. 2005; Fadel and Burk 2010; Zajo et al. 2016; (Villano et al., 2017). Moreover, OxA also modulates synaptic plasticity, the putative correlate of learning and memory, in the hippocampus through coordinated modulation of glutamatergic, GABAergic, noradrenergic, and cholinergic signaling (Selbach et al. 2004).

Prior work from our lab and from others has shown a selective age-related loss of orexin neurons (Sawai et al. 2010; Kessler et al. 2011). In addition, previous studies have revealed that aging also correlates with decreased expression of orexin peptides and their receptors (Terao et al. 2002; Zhang et al. 2002; Porkka-Heiskanen et al. 2004; Downs et al. 2007). Ultimately, these phenomena may serve as a correlate to the cognitive dysfunction seen in aging and age-related cognitive disorders such as Alzheimer's disease.

Because of orexin's role in important physiological and behavioral phenomena such as stabilization of sleep/wake states, food intake, addiction, and cognition there is much interest in orexin receptors as potential therapeutic targets (Messina et al., 2016, Chieffi et al., 2017). The two orexin peptides, orexin A (OxA) and orexin B (OxB) act on two G protein-coupled receptors, with the orexin 1 receptor (Ox1R) binding OxA with high affinity and the orexin 2 receptor (Ox2R) binding both OxA and OxB with relatively high affinity (Smart and Jerman 2002; Ammoun et al. 2003; Gotter et al. 2012b; Leonard and Kukkonen 2014). Several single- and dual- orexin receptor antagonists have been developed (Smart et al. 2001; Gotter et al. 2012a; Steiner et al. 2013; Roecker et al. 2016; Skudlarek et al. 2017) but there is a paucity of selective orexin agonists that might have experimental or clinical utility (Mieda and Sakurai 2013; Turku et al. 2017). Administration of the native peptides, meanwhile, is limited by potential peripheral side effects and limited ability to target the brain due to peripheral degradation and the blood-brain barrier. One route that has been suggested for brain delivery of orexins and other neuropeptides is intranasal administration (Hallschmid and Born 2008; Hanson and Frey 2008; Dhuria et al. 2009; Lammers 2011; Spetter and Hallschmid 2015). Intranasal OxA, for example, has been shown to ameliorate attentional deficits produced by sleep deprivation in non-human primates (Deadwyler et al. 2007). Rodent studies have further shown that intranasal OxA increases food intake and locomotor activity (Dhuria et al. 2016). Finally, limited human trials have suggested that intranasal OxA can ameliorate wakefulness, olfactory and cognitive correlates of narcolepsy (Hallschmid and Born 2008; Baier *et al.* 2011; Weinhold *et al.* 2014). Despite these intriguing findings, however, our understanding of the anatomical and neurochemical mechanisms that may underlie the effect of intranasal orexin on cognition and behavior remains extremely limited. Accordingly, the goal of this study was to use immunohistochemistry and in vivo microdialysis to directly examine the effects of intranasal OxA on measures of neuronal activation and neurotransmitter efflux in a rodent model.

Methods

Animals and surgery

Male Fisher 344/Brown Norway F1 (FBN/F1) hybrid rats (3–4 months; Harlan/NIA; RRID: not registered) weighing approximately 250–300g (upon arrival) were used for all experiments. This strain of rats has been used extensively by our lab and others for

neurobiology of aging studies, because they have reduced susceptibility to many of the non-neurological age-related complications (e.g., intraperitoneal tumors) seen in other strains, even well into the 3rd year of life (Lipman et al., 1996, Turturro et al., 1999). Although the current study focuses on young animals, we have previously studied the effects of aging on the orexin system in this strain (Kessler et al., 2011, Stanley and Fadel, 2012, Hagar et al., 2017) and are currently examining the effects of intranasal orexin in aged animals; therefore, we selected the FBN/F1 strain to facilitate comparisons with prior and ongoing work. All animals were housed in an environmentally controlled animal facility and kept on a 12:12 light: dark cycle with lights on at 07:00 hours. Animals were allowed standard rat chow and water *ad libitum*. All experiments were performed during the light phase with each experiment starting at least 1 hour after the start of the light phase and ending at least 1 hour before the start of the dark phase. Animal care and use practices, including rationale for use and number of animal subjects, were performed in accordance with protocols written under the guidelines of the National Institutes of Health Guide for the Care and Use of Laboratory Animals and approved by the Institutional Animal Care and Use Committee at the University of South Carolina (Animal Use Protocol #2248). Measures taken to minimize animals' suffering include careful monitoring of anesthesia depth during surgery, administration of analgesics to ease post-operative pain (see below), and using a within-subjects multi-session design for in vivo microdialysis (one session with saline control; one session with intranasal OxA) so each animal served as its own control in these experiments, thus reducing the numbers of animals required to achieve equivalent statistical power.

The first author (CBC) performed the methods herein, including group assignment, with the exception of the immunohistochemistry experiments within the brainstem, which were conducted by HF. The individual conducting the cell counts was unaware of the treatment group of the animals (saline vs. OxA) during the counting process. Sample size calculations were not employed, but estimated sample sizes were based on previous studies from our lab using treatment groups of a similar size for immunohistochemistry and microdialysis experiments.

A general timeline for both the c-Fos and microdialysis experiments is depicted in Figure 1. This timeline was repeated for each batch of animals (see below) used for either type of experiment.

Under ketamine/xylazine anesthesia (90/10 mg/kg, ip), animals used for *in vivo* microdialysis received a single guide cannula (BASi West Lafayette, IN, USA) inserted into the PFC at AP +2.8mm, L ±0.5mm, and DV −2.8mm relative to bregma. The guide cannula was anchored in place using two to three skull screws and dental cement. Guide cannula placement was counterbalanced so that left and right hemispheres were equally represented. Upon completion of the surgery, animals were given a single dose of buprenorphine (0.01 mg/kg, sc) to ease post-operative pain and monitored until complete recovery. All animals were allowed at least two full recovery days before habituation in the microdialysis bowls.

Immunohistochemistry

Upon arrival, animals were arbitrarily assigned to receive intranasal administration of either vehicle (50 μl of 0.9% saline) or OxA (50 μl of a 100 μM solution; Enzo Life Sciences).

Animals used for immunohistochemistry were received in three separate batches from NIA (Batch 1, n=6; Batch 2, n=6; Batch 3, n=4). Both treatment conditions were equally represented in each batch (e.g., for Batch 1, three animals received OxA and three animals received saline); however, the order of treatment within a batch of animals was counterbalanced (e.g. for Batch 1, animal 1 received saline, animal 2 received OxA, etc., whereas for Batch 2 animal 1 received OxA, animal 2 received saline, etc.). The individual administering the drug was not blinded to treatment. No additional randomization procedures were used to determine treatment condition or order. All solutions were administered in four 12.5 μl increments over a two-minute period. Each animal was habituated with intranasal saline treatment for 7 days before experimentation. Beginning on day 8, animals received their assigned treatment and were sacrificed two hours later, the time at which c-Fos expression peaks (Kaczmarek 1992). Rats were anesthetized with isoflurane and perfused with phosphate buffered saline (PBS) and 4% paraformaldehyde (PFA). After removal and overnight post-fixation, the brains were coronally sectioned at a 50 μm thickness using a vibratome. A 1:4 serial sectioning method was utilized, allowing for 200μm between each representative section collected. Sections were stored in a 30% sucrose anti-freezing solution at −20°C until use. For single-label immunohistochemistry, free floating sections were incubated with a rabbit-anti c-Fos antibody (1:5000; Millipore; Billerica, MA; catalog No. ABE457; RRID AB_2631318) for 48 h at 4°C followed by a biotinylated donkey anti-rabbit secondary antibody (1:1000; Jackson ImmunoResearch Laboratories Inc.; West Grove, PA; code No. 711-065-152; RRID AB_2340593) for 1.5 h at room temperature (RT), and horseradish peroxidase conjugated streptavidin (1:1600; Jackson ImmunoResearch Laboratories Inc.; West Grove, PA; code No. 016-030-084; RRID AB_2337238) for 1 hour at RT. c-Fos staining was developed with 0.3% hydrogen peroxide and nickel-cobalt enhanced diaminobenzidine to yield blue-black immunopositive nuclei. For dual-label immunohistochemistry, the above steps were followed with incubation in either a goat anti-choline acetyltransferase (ChAT, 1:3000; Millipore; Temecula, CA; catalog No. AB144; RRID AB_90650) or mouse anti-parvalbumin (PV, 1:4000; Sigma; St. Louis, MO; catalog No. P3088; RRID AB_477329) primary antibody for 48 h at 4°C. Secondary and tertiary antibody incubation followed using either unlabeled donkey anti-goat (1:200; Jackson ImmunoResearch Laboratories Inc.; West Grove, PA; code No. 705-005-003; RRID AB_2340384) or unlabeled donkey anti-mouse (1:200; Jackson ImmunoResearch Laboratories Inc.; West Grove, PA; code No. 715-005-150; RRID AB_2340759) for 2 hour at RT, and either goat peroxidase anti-peroxidase (1:500; Jackson ImmunoResearch Laboratories Inc.; West Grove, PA; code No. 123-005-024; RRID AB_2338953) or mouse peroxidase anti-peroxidase (1:500; Jackson ImmunoResearch Laboratories Inc.; West Grove, PA; code No. 223-005-024; RRID AB_2339261) for 1.5 hour at RT. ChAT and PV immunoreactivity were developed with 3% hydrogen peroxide and diaminobenzidine to yield brown immunopositive cell bodies. Sections were mounted onto slides with 0.15% gelatin, dried overnight, dehydrated, delipidated and cover-slipped using DEPEX mounting medium.

In order to perform a qualitative examination of where intranasal OxA distributed within the brain, a subset of animals (n=4) received intranasal administration of either saline or a modified OxA peptide labeled with a green-fluorescent fluorophore (5(6)-FAM-(Glu^1)-OxA

trifluoroacetate salt; BACHEM; Bubendorf, Switzerland). These animals were received in a separate batch from the other immunohistochemistry and microdialysis studies. Due to the descriptive and qualitative nature of this component of the study, no special selection or randomization procedure was used to select these animals. Animals receiving the fluorescein tagged OxA peptide received 50 μL of a 500 μM dose split into four 12.5 μL increments over a two-minute period and were sacrificed thirty minutes post-treatment. This time point was chosen based upon a previous study showing peak appearance of ^{125}I–OxA in the CNS thirty minutes after intranasal delivery (Dhuria et al. 2009). Perfusion and brain sectioning was as described above. Sections were mounted onto slides with 0.15% gelatin, dried overnight, dehydrated only and cover-slipped using Permount mounting medium.

Imaging

Histological experiments for single-labeled (c-Fos) cells, double-labeled (c-Fos + ChAT or PARV) cells, and AChE background staining were visualized using a Nikon E600 microscope fitted with a CoolSNAP digital camera (Roper Scientific, Trenton, NJ, USA). Fluorescence images were visualized using a Nikon E600 microscope or a Leica SP8 multiphoton confocal microscope (Leica Microsystems; Wetzlar, Germany) equipped with LAS AF 3 analysis software (Leica Microsystems; Wetzlar, Germany). Immunoperoxidase photomicrographs were captured using IP Lab Software (Scanalytics; Trenton, NJ, USA). Images were imported into Adobe Photoshop 6.0 (Adobe Systems; San Jose, CA, USA) to adjust the image size and to make minor alterations to contrast and brightness. To indicate the approximate brain region where photomicrographs were obtained, diagrams and schematics of brain regions in the results section were adapted from the third edition of The Rat Brain by Paxinos and Watson (Paxinos and Watson 1998).

Microdialysis and HPLC

Three separate batches of animals were used for the microdialysis experiments (Batch 1, n=2; Batch 2, n=4; Batch 3, n=4). Beginning three days after cannula implantation, animals were habituated in microdialysis bowls for 3–4 days and habituated with intranasal saline for 7 days. On microdialysis days, guide cannula stylets were removed and substituted with a microdialysis probe (BASi, West Lafayette, IN, USA) that extended 2 mm past the guide cannula. Probes were perfused at a 2 μl/min flow rate with artificial cerebrospinal fluid (aCSF, pH 7.4) containing: 150 mM NaCl, 3mM KCl, 1.7mM $CaCl_2$, 0.9 mM $MgCl_2$, and 4.9 mM $_D$-glucose. Neostigmine bromide (50 nM; Sigma) was added to the aCSF to increase recovery of acetylcholine in collected dialysates. Dialysate collection started after a 3 hour discard period. Microdialysis sessions consisted of one hour (4 × 15 minute collections) of baseline collections followed by intranasal vehicle (0.9% saline) or OxA (100 uM; Enzo Life Sciences), administered in a total volume of 50 μl in 12.5 μl increments over a 2-minute period. The individual performing intranasal administration was not blinded to treatment condition. Dialysate collection then continued for two hours (8 × 15 minute collection) post-treatment. Upon collection, dialysates were stored at −80°C until analysis. All animals underwent two separate microdialysis sessions with an off day in-between and experiments were counterbalanced so that half of the animals received vehicle during session one, while the other half received OxA in session one. The day following the last microdialysis session, rats were euthanized and their brains processed for probe placement verification using an

acetylcholinesterase (AChE) background stain. Probe placement verification was performed after all HPLC samples were run for each respective animal. Any probe placement visualized outside the medial PFC excluded the animal from the study.

Each 30 μl dialysate was split prior to analysis by high performance liquid chromatography with electrochemical detection (HPLC-ECD), with 20 μl analyzed for ACh and 10 μl analyzed for glutamate. ACh was analyzed using an HTEC-510 HPLC-ECD (EicomUSA; San Diego, CA, USA). Briefly, 20 μl of each dialysate was loaded into the AC-GEL separation column (2.0 ID × 150mm; EicomUSA) maintained at a constant 33°C in combination with mobile phase (pH 8.5) containing 49.4 mM potassium bicarbonate ($KHCO_3$), 134.3 μM ethylenediaminetetraacetic acid disodium (EDTA-2Na), and 1.23 mM sodium 1-decanesulfonate. After analyte separation, post-column derivatization of ACh was attained through use of an AC-ENYM II enzyme reactor (1.0 ID × 4 mm; EicomUSA) containing acetylcholinesterase and choline oxidase, which generates hydrogen peroxide (H_2O_2) proportional to the amount of ACh present. The H_2O_2 is further broken down and detected on a platinum working electrode with an applied potential of +450 mV. The amount of ACh in each sample was measured by comparison with a three-point external standard curve with values predicted to be in range of the collected dialysates. The limit of detection for this analysis was approximately 5 fmol/injection

Glutamate was analyzed using a CC-32 HPLC-ECD (BASi; West Lafayette, IN, USA) with modifications. First, 10 μl of each dialysate was loaded into the GU-GEL separation column (4.6 ID × 150mm; EicomUSA) in conjunction with a mobile phase (pH 7.2) containing 60 mM ammonium chloride-ammonium hydroxide, 134.3 nM EDTA-2Na, and 686 μM hexadecyltrimethylammonium bromide. After separation, post-column derivatization of glutamate was attained through the use of an E-ENZ enzyme reactor (3.0 ID × 40 mm; EicomUSA) containing glutamate oxidase, which generates H_2O_2 proportional to the amount of glutamate present. The H_2O_2 is further broken down and detected on a 3.0 mm glassy carbon electrode (BASi) coated with a horseradish peroxidase osmium polyvinylpyridine solution (0 mV applied potential). The amount of glutamate in each dialysate was measured by comparison with a three-point standard curve using external standards expected to be in range of the collected dialysates. The limit of detection for this method was approximately 3 fmol/injection.

Statistics and Analysis

For the immunohistochemistry experiments, single-labeled c-Fos and double-labeled (c-Fos + ChAT/PARV) cells were counted within the bounds of a reticle embedded into the eyepiece of the microscope. Staining from each animal was counted using two representative sections at different rostro-caudal levels. Single-labeled c-Fos data were expressed as a density (c-Fos nuclei/mm^2) and analyzed by a two-tailed unpaired t-test (GraphPad Prism 5; GraphPad Software; La Jolla, CA, USA). Double-labeled cells were expressed as the percentage of the total number of ChAT/PARV neurons positive for c-Fos within the reticle and were analyzed by a two-tailed unpaired t-test. A significance cutoff of $p < 0.05$ was used for all analyses.

For the microdialysis experiments, baseline neurotransmitter efflux was obtained during the first four sample collections (i.e. timepoints 1–4) and averaged to yield mean basal efflux. For each sample analyzed, a raw value was obtained and expressed as pmol/20μl for ACh and μmol/l0μl for glutamate. The microdialysis data presented in the graphs are expressed as percent of the average baseline to account for individual variation in basal neurotransmitter efflux. Data were analyzed using two-way repeated-measure ANOVAs (SPSS; IBM; Armonk, NY, USA) with treatment as a within-subjects variable and time as a repeated measure, using a significance cutoff of $p<0.05$. A simple-effects test with Bonferonni corrections was used to probe the source of significant main effects and/or interactions.

Results

Intranasal OxA increases c-Fos expression in select brain regions

Intranasal administration of OxA significantly increased c-Fos expression in multiple brain regions (Table 1; Figure 2a). In the cortex, intranasal OxA increased c-Fos expression in the prelimbic (PrLC; $t_{14}=3.163$, $p=0.0069$), agranular insular (AIC; $t_{14}=3.291$, $p=0.0054$), ventral orbital (VOC; $t_{13}=2.357$, $p=0.0348$), and piriform areas (PirC; $t_{14}=2.259$, $p=0.0404$). Importantly, this effect was not a global phenomenon as intranasal OxA failed to significantly alter c-Fos expression within the claustrum, medial orbital cortex (MOC), and all regions of the hippocampus (Table 1). In fact, there was a strong trend for decreased c-Fos expression in the infralimbic cortex ($t_{14}=2.092$, $p=0.0551$) after intranasal OxA administration. We also considered the possibility that intranasal OxA delivery may alter c-Fos expression within brainstem regions involved in arousal. Indeed, intranasal OxA administration significantly increased c-Fos expression within the pedunculopontine nucleus (PPTg; $t_{13}=2.692$, $p=0.0185$) (Table 1). Below, we also provide corroborating evidence that intranasal OxA delivery reaches more caudal regions of the brainstem, including the spinal trigeminal nucleus (Figure 6c). As an example, density measurements for c-Fos were made using a 0.179 mm × 0.179 mm area in the center of the prelimbic cortex (Figure 2b). Photomicrographs depict increased c-Fos expression in the prelimbic cortex of animals treated with OxA compared to vehicle treatment (Figures 2c,2d). For brainstem c-Fos counts, measurements represent the total number of c-Fos positive nuclei within the entire brain region.

Intranasal OxA decreases c-Fos expression in cortical GABAergic interneurons

To analyze the effects of intranasal OxA on neuronal subpopulations in the cortex, we stained cells for parvalbumin (PV), a marker for fast-spiking GABAergic interneurons in the cortex (Hu et al. 2014). Interestingly, we found that intranasal OxA decreased c-Fos expression in PV neurons of the prelimbic cortex ($t_{14}=3.176$, $p=0.0067$) and ventral orbital cortex ($t_{13}=4.258$, $p=0.0009$). This contrasts with the increase in overall c-Fos expression within these brain regions after intranasal OxA administration (Figure 2a). Data are expressed as the percentage of PV positive neurons also expressing c-Fos (Figure 3a). Single-labeled and double-labeled PV neurons were counted within the same 0.179 mm × 0.179 mm reticle area as c-Fos so that direct comparisons could be established (Figure 3b). Double–labeled PV neurons of the prelimbic cortex are depicted by arrows showing blue-black immunoreactivity for c-Fos and brown immunoreactivity for PV (Figures 3c).

Intranasal OxA increases c-Fos expression in basal forebrain cholinergic neurons

Owing to evidence that OxA activates the BFCS (Eggermann et al. 2001; Fadel et al. 2005; Fadel and Frederick-Duus 2008; Arrigoni et al. 2010; Fadel and Burk 2010), we investigated if intranasal administration of OxA elicited a similar response. Indeed, intranasal OxA increased expression of c-Fos in cholinergic neurons of the vertical limb of the diagonal band (VDBB; t_{14}=5.788, p<0.0001) and ventral pallidum/substantia innominata (VP/SI; t_{14}=3.45, p=0.0039) compared to vehicle. Additionally, there was a strong trend for increased c-Fos expression within the cholinergic neurons of the medial septum (MS; t_{14}=2.133, p=0.0511). Data are expressed as the percentage of choline acetyltransferase (ChAT) positive neurons that also express c-Fos (Figure 4a). Single and double labeled ChAT neurons were counted within the same 0.45mm × 0.45 mm area for each basal forebrain region. As an example, the reticle area in the VDBB is depicted (Figure 4b). Double–labeled ChAT neurons of the VDBB are represented by arrows pointing to the blue-black immunoreactivity for c-Fos and brown immunoreactivity for ChAT (Figures 4b, 4c).

Intranasal OxA increases ACh and glutamate efflux in the PFC

After observing increased c-Fos expression in the PFC, we investigated the effects of intranasal OxA on PFC neurotransmission using *in vivo* microdialysis. Intranasal OxA significantly increased ACh efflux in the PFC as indicated by a significant main effect of TIME ($F_{11,99}$=9.058, p<0.001), a significant main effect of TREATMENT ($F_{1,9}$=14.381, p=0.004), and a significant TIME × TREATMENT interaction ($F_{11,99}$=8.595, p<0.001). Simple effects comparisons with Bonferonni corrections revealed that 100 μM OxA significantly increased ACh efflux compared to vehicle from collections five through nine (all t_9 > 2.93; all p<0.05). Efflux of ACh after intranasal OxA treatment peaked during collection five (15 minutes post-OxA) at approximately 233% of baseline and remained significantly elevated for more than one hour when compared with ACh efflux after treatment with intranasal saline (Figure 5a).

Intranasal OxA also significantly increased glutamate efflux in the PFC compared to vehicle as specified by a significant TIME × TREATMENT interaction ($F_{11,99}$=2.128, p=0.025) although there were no significant main effects of TIME ($F_{11,99}$=1.008, p=0.445) or TREATMENT ($F_{1,9}$=2.866, p=0.125). Simple effects comparisons with Bonferonni corrections indicated significantly increased levels of glutamate from time points five through seven (all t_9 >2.370; all p<0.05). After intranasal OxA administration, significantly increased glutamate efflux was observed during collection five and peaked at collection seven (45 minutes post-OxA) with a maximum efflux around 133% of baseline (Figure 5b).

Probe placement verification via acetylcholinesterase background staining stain revealed that the 2 mm active membrane portion of the dialysis probe was centered in the prelimbic portion of the PFC with a small degree of overlap dorsally into the anterior cingulate cortex or ventrally into infralimbic portion of the prefrontal cortex (Figure 5c.)

Intranasal 5(6)-FAM-(Glu^1)-Hypocretin-1 administration

To visually assess the possible modes by which intranasal OxA enters the brain and to provide qualitative supporting evidence for the above results, we intranasally administered a

fluorescein tagged OxA peptide (5(6)-FAM-(Glu¹)-Hypocretin-1). This ultimately revealed a distribution of the peptide to both rostral and caudal brain regions. Prior work has suggested that intranasally delivered peptides reach the brain via diffusion along sensory trigeminal pathways (Hanson and Frey 2008; Chapman et al. 2013; Spetter and Hallschmid 2015; Meredith et al. 2015). Therefore, we visualized delivery of the fluorescein tagged peptide in the principal sensory and spinal subdivisions of the trigeminal nucleus (Figures 6a, 6b), the sources of somatosensory innervation of the olfactory mucosa. The fluorescein-tagged OxA peptide was also detected in cortical regions, including the medial PFC (Figures 6c, 6d). Due to the qualitative nature of these experiments, a relatively modest treatment size was used (n=4). This pattern of fluorescence was not observed following intranasal vehicle (saline) administration (n=4).

Discussion

Collectively, these experiments demonstrate that intranasal OxA administration increased c-Fos expression in many, but not all areas of cerebral cortex, basal forebrain, and brainstem. The selective nature of OxA-elicited neuronal activation was further demonstrated by a limited phenotypic analysis of these effects, which revealed increased activation of basal forebrain cholinergic neurons but decreases in Fos expression in GABAergic, PV+ interneurons in prelimbic and ventral orbital cortices. Additionally, our microdialysis results demonstrate that intranasal OxA administration rapidly and significantly increases ACh and glutamate within the PFC, an area important for multiple aspects of executive and cognitive function. Thus, in our rodent model, intranasal OxA proved effective at reaching the brain and modulating the activity of multiple brain regions and neurotransmitter systems that mediate cognition and behavior.

Effects of intranasal OxA on c-Fos expression

Orexin regulation of PFC activity has been well-documented. Orexin neurons project robustly to the medial PFC where they enhance neurochemical, electrophysiological and behavioral correlates of attention (Fadel et al. 2005; Lambe et al. 2005; Huang et al. 2006; Vittoz and Berridge 2006). The prelimbic and ventral orbital regions of PFC, where we observed the greatest OxA-elicited neuronal activation, have been implicated in attentional shifting and reversal learning, respectively (Dalley et al. 2004). We also observed robust activation in the agranular insular cortex, part of an area described as putative “interoceptive cortex” due to its role in sensing the organism’s physiological status (Craig and Craig 2002; Avery et al. 2017; Hassanpour et al. 2017). Given the role of orexin neurons in responding to peripheral cues indicative of physiological status, intranasal OxA may facilitate interoceptive processing within the insular region.

Additionally, increased c-Fos expression was also observed in the piriform cortex, a brain region important for olfactory discrimination (Stettler and Axel 2009; Bekkers and Suzuki 2013). Interestingly, there was a (non-significant) trend for decreased c-Fos expression after intranasal OxA in the infralimbic PFC cortex compared to vehicle. This finding is not surprising as divergent functions between the prelimbic and infralimbic PFC have been

described with respect to fear memory, reward processing, and appetitive learning (Vidal-Gonzalez et al. 2006; Ashwell and Ito 2014; Flores et al. 2014; Hayen et al. 2014).

Neuronal activation by intranasal OxA was not limited to the forebrain as we detected increased c-Fos expression within the pedunculopontine tegmental nucleus (PPTg), a part of the reticular activating system that sends projections to PFC (Mesulam et al. 1983; Eckenstein et al. 1988). Importantly, this brain region plays an important role in wakefulness/arousal and attention (Datta et al. 2001; Cyr et al. 2015).

Effects of intranasal OxA on specific neuronal phenotypes

While we observed an overall increase in c-Fos expression in the prelimbic and ventral orbital cortex, we detected the opposite response within PV+ interneurons of these brain regions (Figures 3a), suggesting that intranasal OxA primarily activates glutamatergic neurons in PFC. While it is possible that the overall increases in c-Fos expression reflect activation of other (non-PV+) GABAergic populations, this is unlikely as PV+ GABAergic neurons are the dominant phenotype within the cortex (Kawaguchi and Kubota 1997; Xu et al. 2010; Kelsom and Lu 2013). One potential mechanism may be through OxA activation of PV+ GABAergic neurons in the basal forebrain, which form inhibitory synapses onto PV+ interneurons in the cortex (Henny and Jones 2008). In addition current evidence suggests that orexin activation of PV+ GABAergic neurons in the basal forebrain may be primarily an Ox2R mediated phenomenon (Wu *et al.* 2002; Mieda *et al.* 2011). Whether this pattern of activation extends into other basal forebrain regions that contain more cortically projecting PV+ GABAergic neurons is unknown. Further studies assessing the relative roles of each receptor in the basal forebrain will be vital to understanding orexin regulation of wakefulness, arousal, and attention.

As described above, intranasal OxA induced significant increases in c-Fos expression within the VDBB and VP/SI regions of the basal forebrain. Cholinergic and GABAergic neurons of the VDBB are vital for olfactory memory and spatial memory consolidation (Paolini and McKenzie 1993; Lecourtier et al. 2011), while the collective VP/SI is important for attention, in particular involving reward, motivation, and feeding (Smith et al. 2009). Prior mechanistic descriptions of OxA-basal forebrain interactions have indicated that intrabasalis administration of OxA results in robust increases in cortical ACh release (Fadel et al. 2005). Furthermore, the basal forebrain appears to be an important site for OxA modulation of cholinergic-dependent attentional functions (Boschen et al. 2009; Fadel and Burk 2010; Zajo et al. 2016).

Mechanistic considerations for neuronal activation and neurotransmission

The effects of intranasal OxA administration on c-Fos are corroborated by our effects seen through *in-vivo* microdialysis. In summary, intranasal OxA significantly increased both acetylcholine and glutamate efflux within the PFC. The Ox1R and Ox2R are both expressed in the basal forebrain (Marcus et al. 2001). While direct receptor mechanisms involving intranasal OxA administration cannot be determined from this study, prior studies indicate that our effects may primarily be an Ox1R-mediated phenomenon. For example, intrabasalis administration of OxA elicits a greater response on somatosensory cortical ACh release than

OxB (Dong et al. 2006). Studies from our lab corroborate this finding as the specific Ox1R antagonist SB-334867 block stimulated ACh release during feeding (Frederick-Duus et al. 2007). Still, it is possible that the Ox2R plays a large role in the effects mediated by intranasal OxA administration as previous work using *in vitro* electrophysiology has reported that OxB is as effective as OxA at exciting basal forebrain cholinergic neurons (Eggermann et al. 2001). Importantly, the large increases in ACh efflux (233% of baseline) we observed translate to previous work showing that high levels of ACh in the hippocampus and neocortex set the dynamics for increased attention (Hasselmo and McGaughy 2004).

We also observed significant, although less robust, increases in PFC glutamate efflux after intranasal OxA administration. From a mechanistic standpoint, this effect can arise from a variety of sources. Directly, intranasal OxA may be acting locally within the PFC as orexin receptors are expressed in this brain region (Hervieu et al. 2001; Marcus et al. 2001) and OxA has been shown stimulate presynaptic glutamate release in the PFC (Lambe et al. 2007). Visualization of (5(6)-FAM-(Glu^1)-Hypocretin-1) in the PFC supports this notion (Figures 6c and d). Indirectly, the increases in cortical glutamate efflux that we observed could also come from excitation of glutamatergic thalamocortical synapses originating from the paraventricular nucleus (Lambe et al. 2005; Huang et al. 2006) or possibly from the orexin neurons that colocalize glutamate (Rosin et al. 2003). The latter possibility seems unlikely, however, as we observed no differences in c-Fos expression in orexin labeled neurons between intranasal vehicle and intranasal OxA treated animals (data not shown).

In animal models, aging is associated with reductions in the number of orexin-positive neurons and other markers of orexinergic transmission (Terao et al. 2002; Porkka-Heiskanen et al. 2004; Kessler et al. 2011). Clinical data suggests that orexin deficits also accompany age-related cognitive disorders, including Alzheimer's disease (Thannickal et al. 2000; Thannickal et al. 2009; Fronczek et al. 2012). In addition, narcolepsy (particularly with cataplexy) is the clearest example of a human disorder accompanied by orexin cell loss (Nishino et al. 2000; Siegel 1999), and several lines of evidence suggest that narcoleptic patients exhibit subtle cognitive—particularly attentional—deficits even during periods of apparently normal wakefulness (Rieger et al. 2003; Naumann et al. 2006), suggesting a role of orexin in cognitive function. As shown in the current study, the ability of intranasal OxA to rapidly target the brain and activate brain regions and neurotransmitter systems that support cognition provides mechanistic evidence for the potential therapeutic utility of this approach. Further work is necessary to further elucidate the receptor mechanisms underlying this phenomenon and to demonstrate its efficacy in models of aging and age-related disorders. Importantly, this phenomenon also suggests that the observable effects of intranasal OxA on neurotransmission may be present in cognitive disorders that show reduced numbers of orexin neurons such as narcolepsy and Alzheimer's disease (Thannickal et al. 2000; Thannickal et al. 2009; Fronczek et al. 2012).

Conclusion

In summary, intranasal OxA activates brain regions and neurotransmitter systems that represent the neural substrates of attention, learning, and memory. OxA activates Ox1R and Ox2R, and both of these receptors may contribute to stimulation of cortical ACh and

glutamate release during intranasal OxA administration. Further experimentation using intranasal OxB will help to define the roles for these receptors more clearly. Together, these neurochemical correlates highlight key systems that underlie the cognitive effects of intranasal OxA and suggest that intranasal OxA may be a viable treatment option for cognitive dysfunction.

Acknowledgments

This work was supported by grants from the National Institutes of Health (R01AG050518; JRF), the University of South Carolina SPARC Graduate Research Program (CBC) and the University of South Carolina Magellan Scholars Program (HF). The authors thank Meredith Calva for valuable assistance with artwork.

List of abbreviations used in text

ACh	acetylcholine
AChE	acetylcholinesterase
aCSF	artificial cerebrospinal fluid
AIC	agranular insular cortex
BFCS	basal forebrain cholinergic system
ChAT	choline acetyltransferase
Cl	claustrum
FBN/F1	Fischer 344-Brown Norway/F1 hybrid
HDBB	horizontal limb of the diagonal band of Broca
ILC	infralimbic cortex
LH/PFA	lateral hypothalamus/perifornical area
MOC	medial orbital cortex
MS	medial septum
NaCl	sodium chloride
Ox1R	orexin-1-receptor
Ox2R	orexin-2-receptor
OxA	orexin-A
OxB	orexin-B
PBS	phosphate buffered saline
PFA	paraformaldehyde
PFC	prefrontal cortex

PirC	piriform cortex
PPTg	pedunculopontine nucleus
PrLC	prelimbic cortex
PV	parvalbumin
RRID	Research Resource Identifier
SpTrN	spinal trigeminal nucleus
VDBB	vertical limb of the diagonal band of Broca
VOC	ventral orbital cortex
VP/SI	ventral pallidum/substantia innominata

References

Ammoun S, Holmqvist T, Shariatmadari R, Oonk HB, Detheux M, Parmentier M, Akerman KE, Kukkonen JP. Distinct recognition of OX1 and OX2 receptors by orexin peptides. J Pharmacol Exp Ther. 2003; 305:507–514. [PubMed: 12606634]

Arrigoni E, Mochizuki T, Scammell TE. Activation of the basal forebrain by the orexin/hypocretin neurones. Acta Physiol. 2010; 98:223–235.

Ashwell R, Ito R. Excitotoxic lesions of the infralimbic, but not prelimbic cortex facilitate reversal of appetitive discriminative context conditioning: the role of the infralimbic cortex in context generalization. Front. Behav. Neurosci. 2014; 8:63. [PubMed: 24616678]

Avery JA, Gotts SJ, Kerr KL, Burrows K, Ingeholm JE, Bodurka J, Martin A, Kyle Simmons W. Convergent gustatory and viscerosensory processing in the human dorsal mid-insula. Hum. Brain Mapp. 2017; 38:2150–2164. [PubMed: 28070928]

Baier PC, Hallschmid M, Seeck-Hirschner M, Weinhold SL, Burkert S, Diessner N, Göder R, Aldenhoff JB, Hinze-Selch D. Effects of intranasal hypocretin-1 (orexin A) on sleep in narcolepsy with cataplexy. Sleep Med. 2011; 12:941–946. [PubMed: 22036605]

Bekkers JM, Suzuki N. Neurons and circuits for odor processing in the piriform cortex. Trends Neurosci. 2013; 36:429–38. [PubMed: 23648377]

Boschen KE, Fadel JR, Burk JA. Systemic and intrabasalis administration of the orexin-1 receptor antagonist, SB-334867, disrupts attentional performance in rats. Psychopharmacology (Berl). 2009; 206:205–213. [PubMed: 19575184]

Chapman CD, Frey WH, Craft S, Danielyan L, Hallschmid M, Schiöth HB, Benedict C. Intranasal Treatment of Central Nervous System Dysfunction in Humans. Pharm. Res. 2013; 30:2475–2484. [PubMed: 23135822]

Chieffi S, Carotenuto M, Monda V, Valenzano A, Villano I, Precenzano F, Tafuri D, Salerno M, Filippi N, Nuccio F, Ruberto M, De Luca V, Cipolloni L, Cibelli G, Mollica MP, Iacono D, Nigro E, Monda M, Messina G, Messina A. Orexin System: The Key for a Healthy Life. Frontiers in physiology. 2017; 8:357. [PubMed: 28620314]

Craig, aD, Craig, aD. How do you feel? Interoception: the sense of the physiological condition of the body. Nat. Rev. Neurosci. 2002; 3:655–666. [PubMed: 12154366]

Cyr M, Parent MJ, Mechawar N, Rosa-Neto P, Soucy J-P, Clark SD, Aghourian M, Bedard M-A. Deficit in sustained attention following selective cholinergic lesion of the pedunculopontine tegmental nucleus in rat, as measured with both post-mortem immunocytochemistry and in vivo PET imaging with [18F]fluoroethoxybenzovesamicol. Behav. Brain Res. 2015; 278:107–114. [PubMed: 25257103]

Dalley JW, Cardinal RN, Robbins TW. Prefrontal executive and cognitive functions in rodents: Neural and neurochemical substrates. Neurosci. Biobehav. Rev. 2004; 28:771–784. [PubMed: 15555683]

Datta S, Spoley EE, Patterson EH. Microinjection of glutamate into the pedunculopontine tegmentum induces REM sleep and wakefulness in the rat. Am. J. Physiol. Regul. Integr. Comp. Physiol. 2001; 280:R752–9. [PubMed: 11171654]

Deadwyler SA, Porrino L, Siegel JM, Hampson RE. Systemic and nasal delivery of orexin-A (Hypocretin-1) reduces the effects of sleep deprivation on cognitive performance in nonhuman primates. J. Neurosci. 2007; 27:14239–47. [PubMed: 18160631]

Dhuria SV, Hanson LR, Frey WH. Intranasal drug targeting of hypocretin-1 (orexin-A) to the central nervous system. J. Pharm. Sci. 2009; 98:2501–2515. [PubMed: 19025760]

Dhuria SV, Fine JM, Bingham D, Svitak AL, Burns RB, Baillargeon AM, Panter SS, Kazi AN, Frey WH, Hanson LR. Food consumption and activity levels increase in rats following intranasal Hypocretin-1. Neurosci. Lett. 2016; 627:155–159. [PubMed: 27264485]

Dong H, Fukuda S, Murata E, Zhu Z, Higuchi T. Orexins increase cortical acetylcholine release and electroencephalographic activation through orexin-1 receptor in the rat basal forebrain during isoflurane anesthesia. Anesthesiology. 2006; 104:1023–1032. [PubMed: 16645455]

Downs JL, Dunn MR, Borok E, Shanabrough M, Horvath TL, Kohama SG, Urbanski HF. Orexin neuronal changes in the locus coeruleus of the aging rhesus macaque. Neurobiol. Aging. 2007; 28:1286–1295. [PubMed: 16870307]

Eckenstein FP, Baughman RW, Quinn J. An anatomical study of cholinergic innervation in rat cerebral cortex. Neuroscience. 1988; 25:457–474. [PubMed: 2456488]

Eggermann E, Serafin M, Bayer L, Machard D, Saint-Mleux B, Jones BE, Muhlethaler M, Mühlethaler M. Orexins/hypocretins excite basal forebrain cholinergic neurones. Neuroscience. 2001; 108:177–181. [PubMed: 11734353]

Fadel J, Burk JA. Orexin/hypocretin modulation of the basal forebrain cholinergic system: Role in attention. Brain Res. 2010; 1314:112–123. [PubMed: 19699722]

Fadel J, Frederick-Duus D. Orexin/hypocretin modulation of the basal forebrain cholinergic system: Insights from in vivo microdialysis studies. Pharmacol Biochem Behav. 2008; 90:156–162. [PubMed: 18281084]

Fadel J, Pasumarthi R, Reznikov LR. Stimulation of cortical acetylcholine release by orexin A. Neuroscience. 2005; 130:541–547. [PubMed: 15664710]

Flores A, Valls-Comamala VV, Costa G, Saravia RR, Maldonado R, Berrendero F, Flores A, et al. The Hypocretin/Orexin System Mediates the Extinction of Fear Memories. Neuropsychopharmacology. 2014; 39:1–10.

Frederick-Duus D, Guyton MF, Fadel J. Food-elicited increases in cortical acetylcholine release require orexin transmission. Neuroscience. 2007; 149:499–507. [PubMed: 17928158]

Fronczek R, Geest S van, Frölich M, Overeem S, Roelandse FWC, Lammers GJ, Swaab DF. Hypocretin (orexin) loss in Alzheimer's disease. Neurobiol. Aging. 2012; 33:1642–1650. [PubMed: 21546124]

Gotter AL, Roecker AJ, Hargreaves R, Coleman PJ, Winrow CJ, Renger JJ. Orexin receptors as therapeutic drug targets. Prog. Brain Res. 2012a; 198:163–188. [PubMed: 22813974]

Gotter AL, Webber AL, Coleman PJ, Renger JJ, Winrow CJ. International Union of Basic and Clinical Pharmacology. LXXXVI. Orexin Receptor Function, Nomenclature and Pharmacology. Pharmacol. Rev. 2012b; 64:389–420. [PubMed: 22759794]

Hagar JM, Macht VA, Wilson SP, Fadel JR. Upregulation of orexin/hypocretin expression in aged rats: Effects on feeding latency and neurotransmission in the insular cortex. Neuroscience. 2017; 350:124–132. [PubMed: 28344067]

Hallschmid M, Born J. Revealing the potential of intranasally administered orexin A. Mol Interv. 2008; 8:133–137. [PubMed: 18693191]

Hanson LR, Frey WH. Intranasal delivery bypasses the blood-brain barrier to target therapeutic agents to the central nervous system and treat neurodegenerative disease. Bmc Neurosci. 2008; 9

Hassanpour MS, Simmons WK, Feinstein JS, Luo Q, Lapidus RC, Bodurka J, Paulus MP, Khalsa SS. The Insular Cortex Dynamically Maps Changes in Cardiorespiratory Interoception. Neuropsychopharmacology. 2017 [Epub ahead of print].

Hasselmo ME, McGaughy J. High acetylcholine levels set circuit dynamics for attention and encoding and low acetylcholine levels set dynamics for consolidation. Prog. Brain Res. 2004; 145:207–231. [PubMed: 14650918]

Hayen A, Meese-Tamuri S, Gates A, Ito R. Opposing roles of prelimbic and infralimbic dopamine in conditioned cue and place preference. Psychopharmacology (Berl). 2014; 231:2483–2492. [PubMed: 24429871]

Henny P, Jones BE. Projections from basal forebrain to prefrontal cortex comprise cholinergic, GABAergic and glutamatergic inputs to pyramidal cells or interneurons. Eur. J. Neurosci. 2008; 27:654–670. [PubMed: 18279318]

Hervieu G, Cluderay J, Harrison D, Roberts J, Leslie R. Gene expression and protein distribution of the orexin-1 receptor in the rat brain and spinal cord. Neuroscience. 2001; 103:777–797. [PubMed: 11274794]

Hu H, Gan J, Jonas P. Fast-spiking, parvalbumin+ GABAergic interneurons: From cellular design to microcircuit function. Science. 2014; 345:1255263–1255263. [PubMed: 25082707]

Huang H, Ghosh P, Pol AN van den. Prefrontal cortex-projecting glutamatergic thalamic paraventricular nucleus-excited by hypocretin: a feedforward circuit that may enhance cognitive arousal. J. Neurophysiol. 2006; 95:1656–1668. [PubMed: 16492946]

Kaczmarek L. Expression of c-fos and other genes encoding transcription factors in long-term potentiation. [Review]. Behav Neural Biol. 1992; 57:263–266. [PubMed: 1319707]

Kawaguchi Y, Kubota Y. GABAergic Cell Subtypes and their Synaptic Connections in Rat Frontal Cortex. Cereb Cortex. 1997; 7:476–486. [PubMed: 9276173]

Kelsom C, Lu W. Development and specification of GABAergic cortical interneurons. Cell Biosci. 2013; 3:19. [PubMed: 23618463]

Kessler BA, Stanley EM, Frederick-Duus D, Fadel J. Age-related loss of orexin/hypocretin neurons. Neuroscience. 2011; 178:82–88. [PubMed: 21262323]

Lambe EK, Liu RJ, Aghajanian GK. Schizophrenia, hypocretin (orexin), and the thalamocortical activating system. Schizophr. Bull. 2007; 33:1284–1290. [PubMed: 17656637]

Lambe EK, Olausson P, Horst NK, Taylor JR, Aghajanian GK. Hypocretin and nicotine excite the same thalamocortical synapses in prefrontal cortex: correlation with improved attention in rat. J. Neurosci. 2005; 25:5225–5229. [PubMed: 15917462]

Lammers GJ. Intranasal hypocretin-1: Making sense of scents? Sleep Med. 2011; 12:939–940. [PubMed: 22136855]

Lecourtier L, Vasconcelos AP de, Leroux E, Cosquer B, Geiger K, Lithfous S, Cassel J-C. Septohippocampal pathways contribute to system consolidation of a spatial memory: Sequential implication of gabaergic and cholinergic neurons. Hippocampus. 2011; 21:1277–1289. [PubMed: 20623740]

Leonard CS, Kukkonen JP. Orexin/hypocretin receptor signalling: A functional perspective. 2014

Li J, Hu Z, Lecea L de. The hypocretins/orexins: integrators of multiple physiological functions. Br. J. Pharmacol. 2014; 171:332–50. [PubMed: 24102345]

Lipman RD, Chrisp CE, Hazzard DG, Bronson RT. Pathologic characterization of brown Norway, brown Norway x Fischer 344, and Fischer 344 x brown Norway rats with relation to age. J Gerontol A Biol Sci Med Sci. 1996; 51:B54–59. [PubMed: 8548501]

Marcus JN, Aschkenasi CJ, Lee CE, Chemelli RM, Saper CB, Yanagisawa M, Elmquist JK. Differential expression of orexin receptors 1 and 2 in the rat brain. J. Comp. Neurol. 2001; 435:6–25. [PubMed: 11370008]

Meredith ME, Salameh TS, Banks Wa. Intranasal Delivery of Proteins and Peptides in the Treatment of Neurodegenerative Diseases. AAPS J. 2015; 17:780–787. [PubMed: 25801717]

Messina G, Di Bernardo G, Viggiano A, De Luca V, Monda V, Messina A, Chieffi S, Galderisi U, Monda M. Exercise increases the level of plasma orexin A in humans. Journal of basic and clinical physiology and pharmacology. 2016; 27:611–616. [PubMed: 27665420]

Mesulam MM, Mufson EJ, Wainer BH, Levey AI. Central cholinergic pathways in the rat: An overview based on an alternative nomenclature (Ch1-Ch6). Neuroscience. 1983; 10:1185–1201. [PubMed: 6320048]

Mieda M, Hasegawa E, Kisanuki YY, Sinton CM, Yanagisawa M, Sakurai T. Differential Roles of Orexin Receptor-1 and-2 in the Regulation of Non-REM and REM Sleep. J. Neurosci. 2011; 31:6518–6526. [PubMed: 21525292]

Mieda M, Sakurai T. Orexin (Hypocretin) receptor agonists and antagonists for treatment of sleep disorders: Rationale for development and current status. CNS Drugs. 2013; 27:83–90. 2013. [PubMed: 23359095]

Naumann A, Bellebaum C, Daum I. Cognitive deficits in narcolepsy. J. Sleep Res. 2006; 15:329–338. [PubMed: 16911036]

Nishino S, Ripley B, Overeem S, Lammers GJ, Mignot E. Hypocretin (orexin) deficiency in human narcolepsy. Lancet. 2000; 355:39–40. [PubMed: 10615891]

Paolini AG, McKenzie JS. Effects of lesions in the horizontal diagonal band nucleus on olfactory habituation in the rat. Neuroscience. 1993; 57:717–724. [PubMed: 8309533]

Paxinos, G., Watson, C. The rat brain in stereotaxic coordinates. San Diego, CA: Academic Press; 1998.

Peyron C, Tighe DK, Pol aN van den, Lecea L de, Heller HC, Sutcliffe JG, Kilduff TS. Neurons containing hypocretin (orexin) project to multiple neuronal systems. J. Neurosci. 1998; 18:9996–10015. [PubMed: 9822755]

Porkka-Heiskanen T, Alanko L, Kalinchuk A, Heiskanen S, Stenberg D. The effect of age on prepro-orexin gene expression and contents of orexin A and B in the rat brain. Neurobiol. Aging. 2004; 25:231–238. [PubMed: 14749141]

Rieger M, Mayer G, Gauggel S. Attention deficits in patients with narcolepsy. Sleep. 2003; 26:36–43. [PubMed: 12627730]

Roecker AJ, Cox CD, Coleman PJ. Orexin Receptor Antagonists: New Therapeutic Agents for the Treatment of Insomnia. J. Med. Chem. 2016; 59:504–530. [PubMed: 26317591]

Rosin DL, Weston MC, Sevigny CP, Stornetta RL, Guyenet PG. Hypothalamic orexin (Hypocretin) neurons express vesicular glutamate transporters VGLUT1 or VGLUT2. J. Comp. Neurol. 2003; 465:593–603. [PubMed: 12975818]

Sawai N, Ueta Y, Nakazato M, Ozawa H. Developmental and aging change of orexin-A and -B immunoreactive neurons in the male rat hypothalamus. Neurosci. Lett. 2010; 468:51–55. [PubMed: 19857552]

Selbach O, Doreulee N, Bohla C, Eriksson K, Sergeeva O, Poelchen W, Brown R, Haas H. Orexins/hypocretins cause sharp wave- and θ-related synaptic plasticity in the hippocampus via glutamatergic, gabaergic, noradrenergic, and cholinergic signaling. Neuroscience. 2004; 127:519–528. [PubMed: 15262340]

Siegel JM. Narcolepsy: A key role for hypocretins (Orexins). 1999

Skudlarek JW, DiMarco CN, Babaoglu K, Roecker AJ, Bruno JG, Pausch MA, O'Brien JA, et al. Investigation of orexin-2 selective receptor antagonists: Structural modifications resulting in dual orexin receptor antagonists. Bioorganic Med. Chem. Lett. 2017; 27:1364–1370.

Smart D, Jerman JC. The physiology and pharmacology of the orexins. 2002

Smart D, Sabido-David C, Brough SJ, Jewitt F, Johns A, Porter RA, Jerman JC. SB-334867-A: the first selective orexin-1 receptor antagonist. Br. J. Pharmacol. 2001; 132:1179–82. [PubMed: 11250867]

Smith KS, Tindell AJ, Aldridge JW, Berridge KC. Ventral pallidum roles in reward and motivation. Behav Brain Res. 2009; 196:155–67. [PubMed: 18955088]

Song CH, Chen XW, Xia JX, Yu ZP, Hu ZA. Modulatory effects of hypocretin-1/orexin-A with glutamate and gamma-aminobutyric acid on freshly isolated pyramidal neurons from the rat prefrontal cortex. Neurosci. Lett. 2006; 399:101–105. [PubMed: 16495001]

Spetter MS, Hallschmid M. Intranasal Neuropeptide Administration To Target the Human Brain in Health and Disease. Mol. Pharm. 2015; 12:2767–2780. [PubMed: 25880274]

Stanley EM, Fadel J. Aging-related deficits in orexin/hypocretin modulation of the septohippocampal cholinergic system. Synapse. 2012; 66:445–452. [PubMed: 22213437]

Steiner MA, Gatfield J, Brisbare-Roch C, Dietrich H, Treiber A, Jenck F, Boss C. Discovery and Characterization of ACT-335827, an Orally Available, Brain Penetrant Orexin Receptor Type1 Selective Antagonist. Chem Med Chem. 2013; 8:898–903. [PubMed: 23589487]

Stettler DD, Axel R. Representations of Odor in the Piriform Cortex. Neuron. 2009; 63:854–864. [PubMed: 19778513]

Terao A, Apte-Deshpande A, Morairty S, Freund YR, Kilduff TS. Age-related decline in hypocretin (orexin) receptor 2 messenger RNA levels in the mouse brain. Neurosci. Lett. 2002; 332:190–194. [PubMed: 12399012]

Thannickal TC, Moore RY, Nienhuis R, Ramanathan L, Gulyani S, Aldrich M, Cornford M, Siegel JM. Reduced number of hypocretin neurons in human narcolepsy. Neuron. 2000; 27:469–474. [PubMed: 11055430]

Thannickal TC, Nienhuis R, Siegel JM. Localized loss of hypocretin (orexin) cells in narcolepsy without cataplexy. Sleep. 2009; 32:993–8. [PubMed: 19725250]

Turku A, Rinne MK, Boije Af Gennäs G, Xhaard H, Lindholm D, Kukkonen JP. Orexin receptor agonist Yan 7874 is a weak agonist of orexin/hypocretin receptors and shows orexin receptor-independent cytotoxicity. PLoS One. 2017; 12

Turturro A, Witt WW, Lewis S, Hass BS, Lipman RD, Hart RW. Growth curves and survival characteristics of the animals used in the Biomarkers of Aging Program. J Gerontol A Biol Sci Med Sci. 1999; 54:B492–501. [PubMed: 10619312]

Vidal-Gonzalez I, Vidal-Gonzalez B, Rauch SL, Quirk GJ. Microstimulation reveals opposing influences of prelimbic and infralimbic cortex on the expression of conditioned fear. Learn. Mem. 2006; 13:728–33. [PubMed: 17142302]

Villano I, Messina A, Valenzano A, Moscatelli F, Esposito T, Monda V, Esposito M, Precenzano F, Carotenuto M, Viggiano A, Chieffi S, Cibelli G, Monda M, Messina G. Basal Forebrain Cholinergic System and Orexin Neurons: Effects on Attention. Frontiers in behavioral neuroscience. 2017; 11:10. [PubMed: 28197081]

Vittoz NM, Berridge CW. Hypocretin/Orexin Selectively Increases Dopamine Efflux within the Prefrontal Cortex: Involvement of the Ventral Tegmental Area. Neuropsychopharmacology. 2006; 31:384–395. [PubMed: 15988471]

Weinhold SL, Goder R, Baier PC. Improvement of divided attention in narcolepsy by intranasal orexin-A. J. Sleep Res. 2014; 23:291.

Wu M, Zhang Z, Leranth C, Xu C, Pol AN van den, Alreja M. Hypocretin increases impulse flow in the septohippocampal GABAergic pathway: implications for arousal via a mechanism of hippocampal disinhibition. J. Neurosci. 2002; 22:7754–65. [PubMed: 12196599]

Xu X, Roby KD, Callaway EM. Immunochemical characterization of inhibitory mouse cortical neurons: three chemically distinct classes of inhibitory cells. J. Comp. Neurol. 2010; 518:389–404. [PubMed: 19950390]

Zajo KN, Fadel JR, Burk JA. Orexin A-induced enhancement of attentional processing in rats: role of basal forebrain neurons. Psychopharmacology (Berl). 2016; 233:639–647. [PubMed: 26534765]

Zhang JH, Sampogna S, Morales FR, Chase MH. Age-related changes in hypocretin (orexin) immunoreactivity in the cat brainstem. Brain Res. 2002; 930:206–211. [PubMed: 11879811]

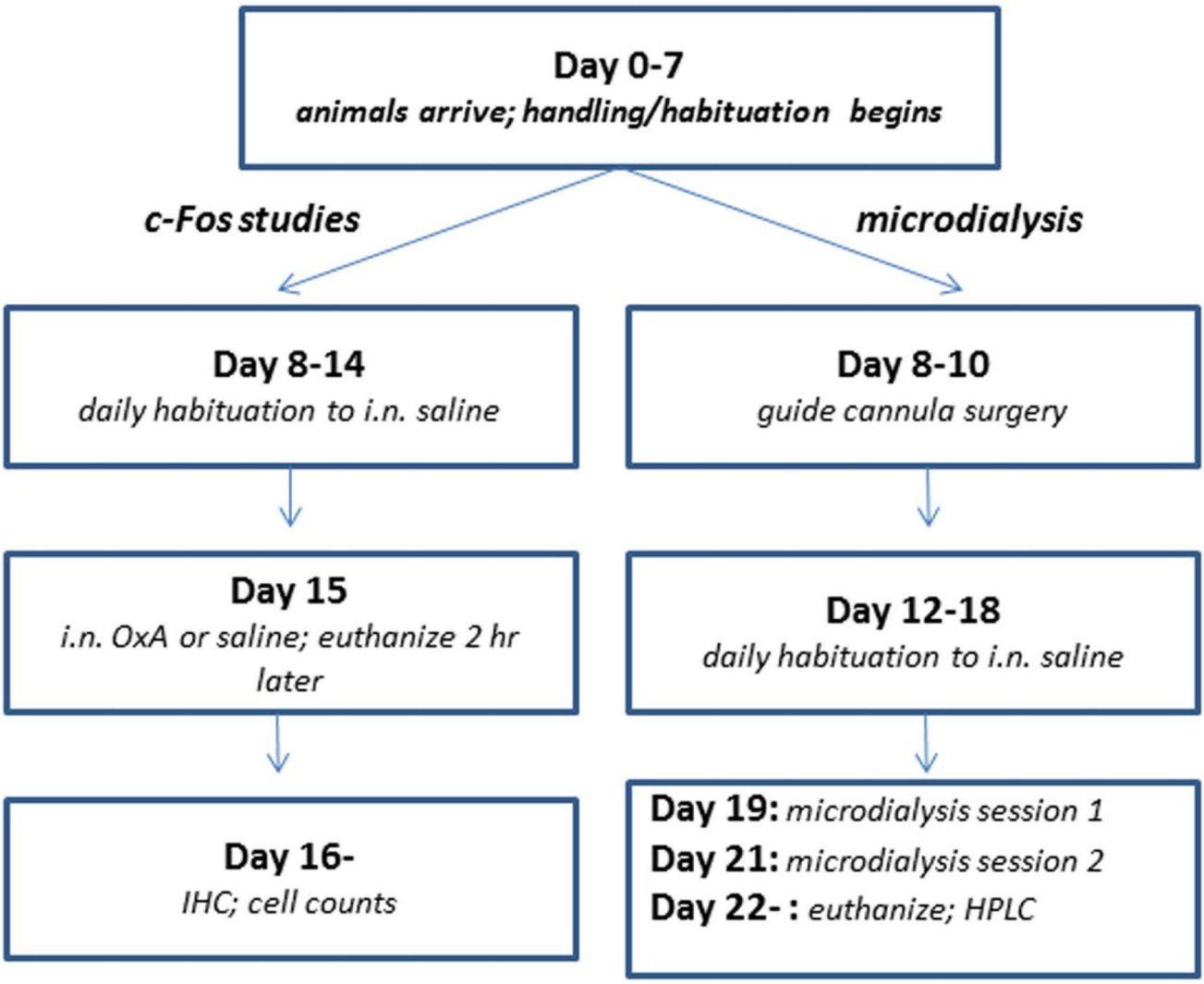

Fig. 1.

General experimental timeline. Day 0 represents the day of arrival of each batch of animals at the University of South Carolina School of Medicine vivarium. Handling and habituation of the rats began the following day. After one week, animals were assigned to either the c-Fos expression or in vivo microdialysis experimental groups. For the c-Fos experiments animals received a week of daily habituation to intranasal saline. On the test day (Day 15) each rat received intranasal OxA or saline and was euthanized 2 hr later. Processing of brain tissue, immunohistochemistry, cell counts and data analysis began on Day 16 and proceeded until complete for each batch of rats used for c-Fos analysis. For the in vivo microdialysis experiments, guide cannula surgery was performed during Days 8–10. After several days of recovery, animals received a week of daily habituation to intranasal saline. The first microdialysis session was performed on Day 19 and the second session on Day 21. Half of the rats received OxA in the first session and saline in the second session; the order was reversed for the other half of the rats. On the day following the second microdialysis session (Day 22) the rats were euthanized, their brains processed for histochemical verification of probe placement, and HPLC analysis of dialysate samples began.

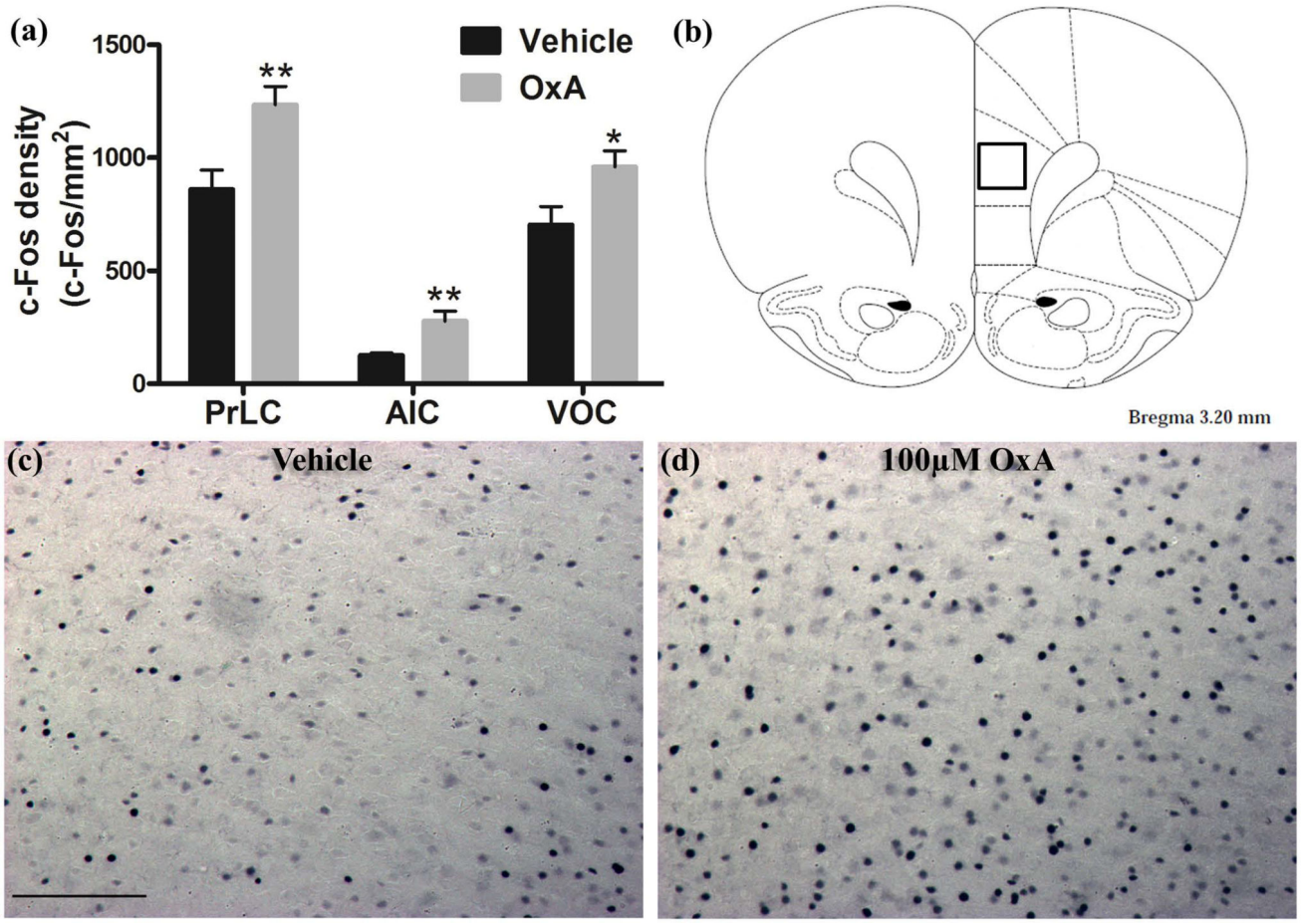

Fig. 2.

Neuronal activation (c-Fos expression density) in cortical brain regions following intranasal OxA administration. (a) Single-labeled c-Fos density for animals treated with intranasal saline (vehicle; PrLC, AIC, VOC, n=8 rats) or intranasal OxA (50 µl, 100 µM; PrLC and AIC, n=8 rats; VOC, n=7 rats). Treatment with intranasal OxA resulted in increased c-Fos expression in neurons of PrLC, AIC, and VOC compared to vehicle treated controls (b) Diagram indicating the approximate location (black-outlined square) within the PrLC for which c-Fos counts and photomicrographs were obtained. (c) Single-label immunohistochemistry for c-Fos shown as blue/black punctate nuclei following acute treatment with intranasal saline. (d) Single-label immunohistochemistry for c-Fos following acute treatment with intranasal OxA. A clear increase in c-Fos expression density is seen in the OxA treatment group (d) compared to vehicle controls (c). Abbreviations: OxA, orexin-A; PrLC, prelimbic prefrontal cortex; AIC, agranular insular cortex; VOC, ventral orbital cortex. Scale bar represents approximately 100 µm (c, d). Error bars represent SEM. **p<0.01, *p<0.05

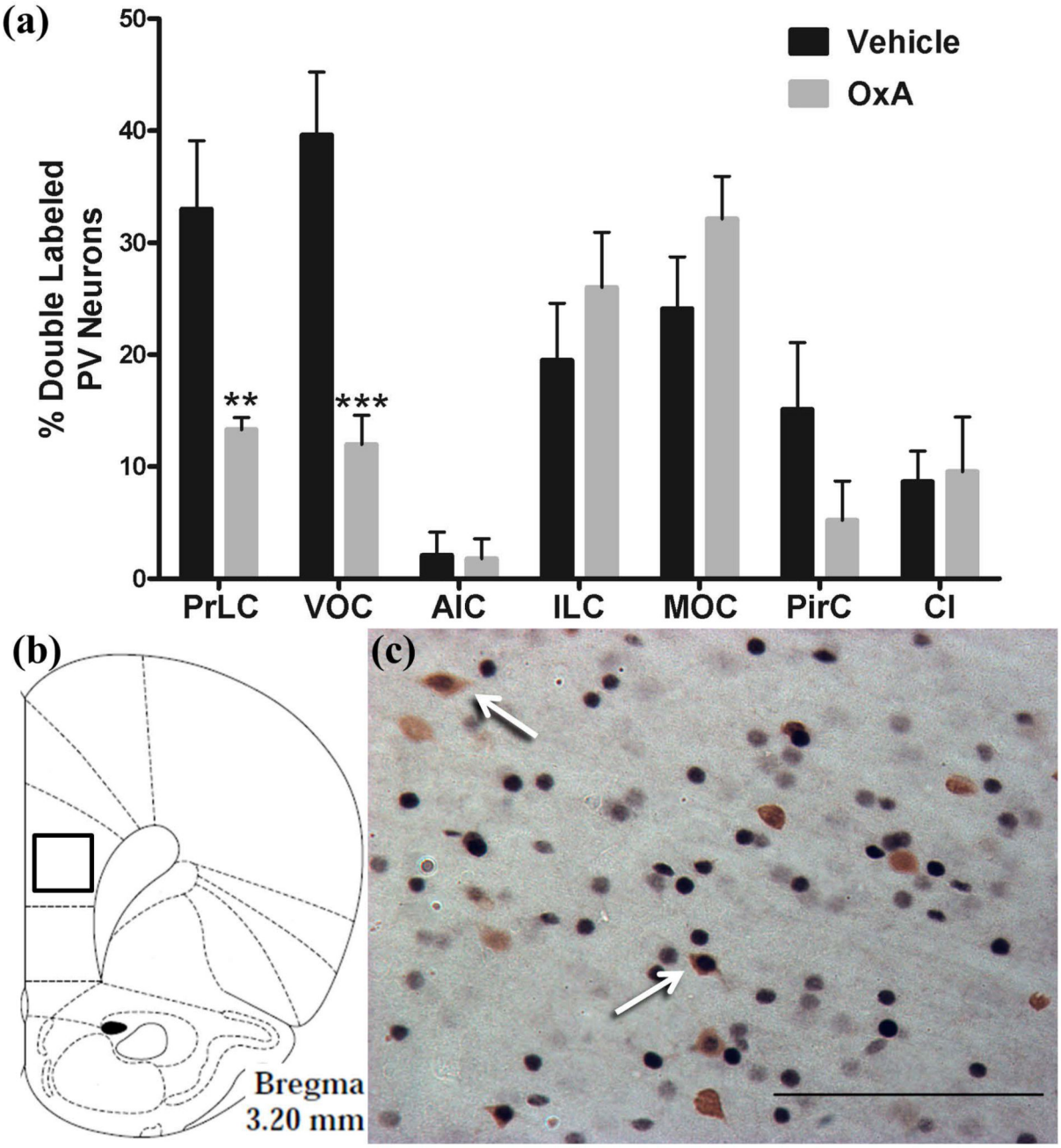

Fig. 3.

Activation of PV-positive GABAergic interneurons in cortical brain regions after intranasal OxA administration. (a) Percentage of double-labeled (c-Fos/PV) neurons relative to the total number of PV neurons within the PrLC, VOC, AIC, ILC, MOC, PirC, and Cl after treatment with intranasal saline (vehicle; all regions, n=8 rats) or intranasal OxA (50 μl, 100 μM; PrLC, AIC, ILC, PirC, and Cl, n=8 rats; VOC and MOC, n=7 rats). Intranasal OxA significantly increased the percentage of dual-labeled PV neurons in the PrLC and VOC. Other cortical regions including the AIC, ILC, MOC, and PirC, as well as the subcortical claustrum, did not show significant differences between treatment groups. (b) Schematic

indicating the approximate location (black-outlined square) within the PrLC where c-Fos/PV counts and photomicrographs were obtained. (c) Typical dual-label immunohistochemistry for c-Fos (blue/black) and PV (brown) neurons within the PrLC (arrows). Abbreviations: PV, parvalbumin; OxA, orexin-A; PrLC, prelimbic prefrontal cortex; VOC, ventral orbital cortex; AIC, agranular insular cortex; ILC, infralimbic prefrontal cortex; MOC, medial orbital cortex; PirC, piriform cortex; Cl, Claustrum. Scale bar represents approximately 100 μm (c). Error bars represent SEM. ***$p<0.001$, **$p<0.01$

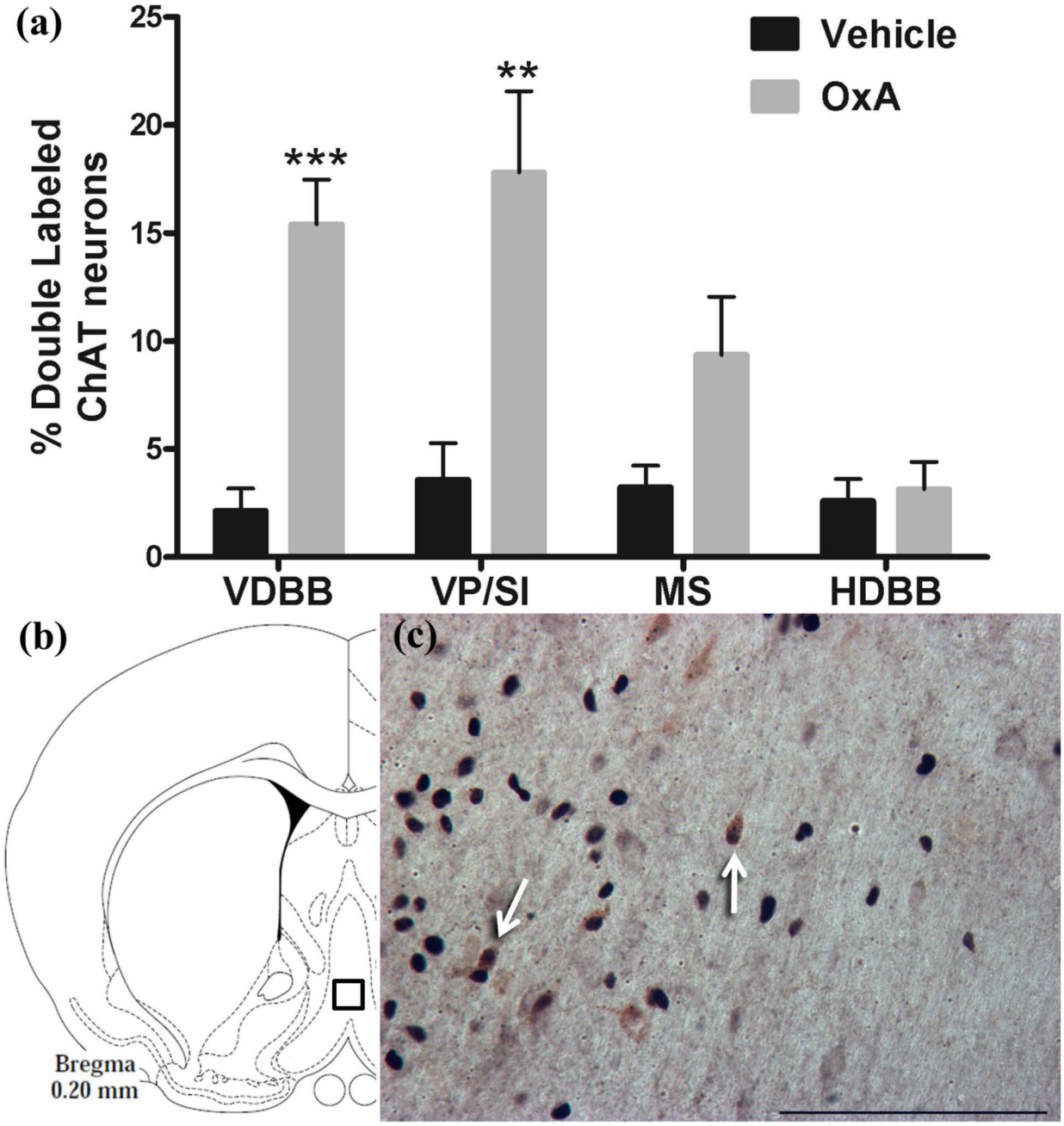

Fig. 4.

Activation of cholinergic neurons in the basal forebrain by intranasal OxA administration. (a) Percentage of double-labeled (c-Fos/ChAT) neurons relative to the total number of ChAT positive neurons within the VDBB, VP/SI, MS, and HDBB after treatment with intranasal saline (vehicle; all regions, n=8 rats) or intranasal OxA (50 μl, 100 μM; all regions, n=8 rats). Intranasal OxA significantly increased the percentage of dual-labeled ChAT neurons in the VDBB and VP/SI compared to vehicle treated controls. (b) Schematic indicating the approximate location (black-outlined square) within the VDBB where c-Fos/ChAT counts and photomicrographs were obtained. (c) Typical dual-label immunohistochemistry for c-

Fos (blue/black) and ChAT (brown) neurons within the VDBB (arrows). Abbreviations: OxA, orexin-A; ChAT, choline acetyltransferase; VDBB, vertical limb of the diagonal band; VP/SI, ventral pallidum/substantia innominata; MS, medial septum; HDBB, horizontal limb of the diagonal band. Scale bar represents approximately 100 μm (c). Error bars represent SEM. ***$p<0.001$, **$p<0.01$

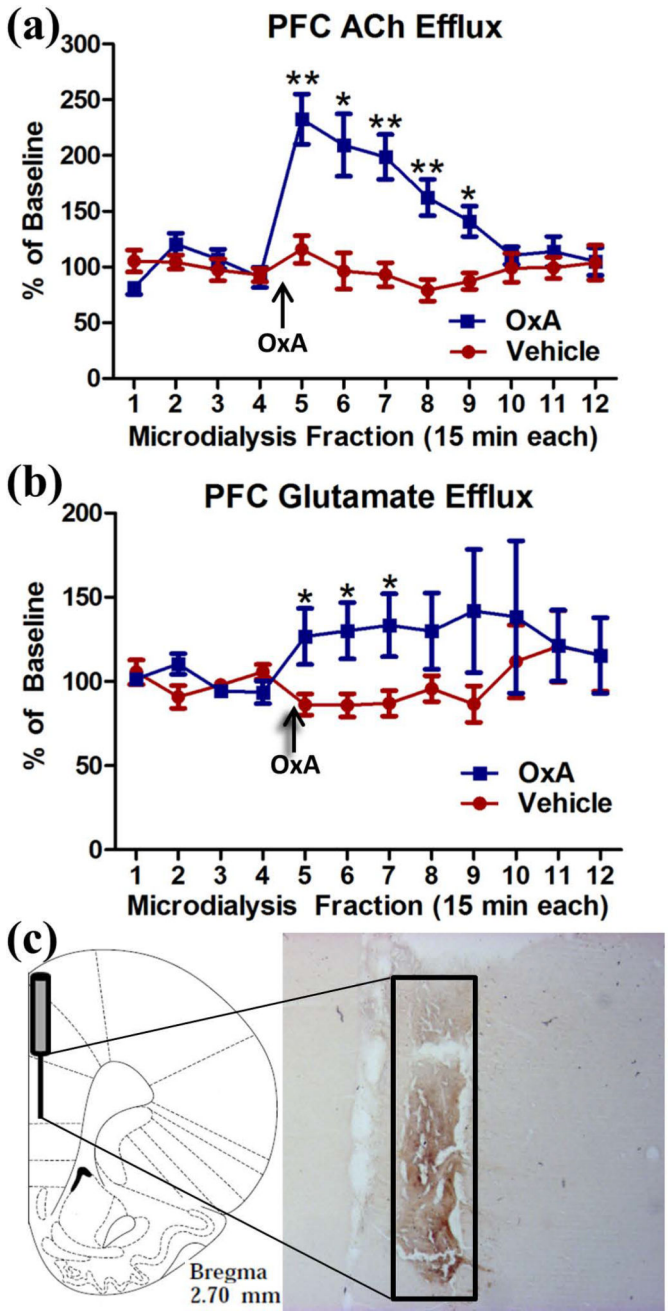

Fig. 5.

Effect of intranasal OxA administration on ACh and glutamate efflux in the PFC. (a) Intranasal OxA (50 μl, 100 μM; n=10 rats) treatment after baseline collections (arrow) significantly increased ACh efflux compared to intranasal vehicle (saline; n=10 rats). A significant increase in ACh efflux was observed from time points five through nine versus vehicle (b) Intranasal OxA (arrow; n=10 rats) also significantly increased glutamate efflux within the prefrontal cortex compared to treatment with intranasal saline. The significant effect lasted from time points five through eight versus vehicle treatment. (c) Diagram indicating the approximate probe placement within the PFC for each of the animals that

underwent microdialysis. Typical probe placement in the PFC is indicated on AChE background-stained section from an animal that underwent two microdialysis sessions. Abbreviations: PFC, prefrontal cortex; ACh, acetylcholine; in, intranasal; OxA, orexin-A. Error bars represent SEM. **p<.01, *p<.05

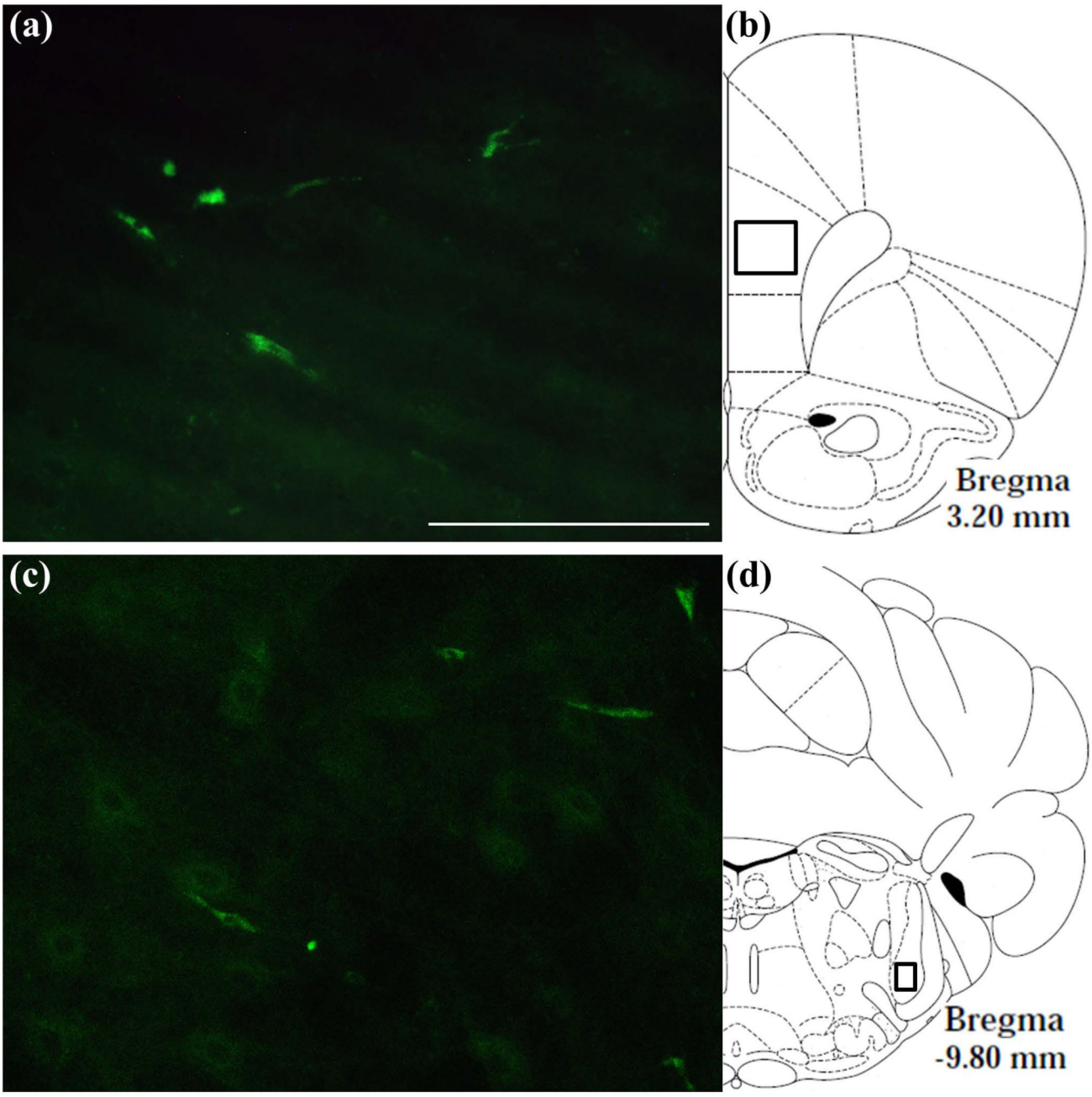

Fig. 6.

Localization of a green-fluorescent tagged OxA peptide in the brain after intranasal administration. (a) Typical distribution of the fluorescent-tagged OxA peptide (50 μl, 500 μM) in the PrLC after intranasal administration. Green fluorescence indicates the appearance of the labeled peptide in the PrLC. (b) Schematic indicating the approximate location (black-outlined square) within the PrLC where fluorescence photomicrographs were obtained. (c) Typical distribution of the fluorescent-tagged OxA peptide in the SpTrN. (d) Schematic indicating the approximate location (black-outlined square) within the SpTrN where fluorescence photomicrographs were obtained. Abbreviations: OxA, orexin-A; PrLC,

prelimbic prefrontal cortex; SpTrN, spinal trigeminal nucleus. Scale bar approximately 100 μm.

Table 1

Comparison of c-Fos densities (nuclei/mm^2) for each brain region listed after intranasal vehicle (saline) or intranasal OxA (50 μl, 100 μM) administration. In the cerebral cortex, OxA significantly increased c-Fos expression in the piriform, agranular cortex, prelimbic, and ventral orbital cortices compared to intranasal saline. There was also a strong trend (p=0.0551) for decreased c-Fos expression in the infralimbic cortex after intranasal OxA administration compared to vehicle. The medial orbital cortex, perirhinal cortex, and hippocampal brain regions yielded no significant differences between the two treatment groups. Among brainstem regions, the pedunculopontine nucleus was the only ares where intranasal OxA administration significantly increased c-Fos expression. Counts for c-Fos positive nuclei in the pedunculopontine nucleus are reported as the total number in the entire region. There were n=8 animals per treatment group with the exception of the vehicle group for the PPTg and the OxA group for the ventral and medial orbital cortices. These three treatment groups are represented by n=7 rats/group. **p<.01, *p<.05

c-Fos density (nuclei/mm^2)		
Brain Region	**Vehicle**	**100 uM OxA**
Piriform Cortex *	582 ± 38.24, n=8	777.3 ± 77.55, n=8
Agranular Insular Cortex **	125 ± 10.23, n=8	277.3 ± 45.15, n=8
Prelimbic Cortex **	859.4 ± 86.19, n=8	1234 ± 81.4, n=8
Ventral Orbital Cortex *	703.1 ± 80.97, n=8	959.8 ± 70.45, n=7
Infralimibc Cortex **(p=0.0551)**	890.6 ± 38.27, n=8	714.8 ± 74.8, n=8
Medial Orbital Cortex	609.4 ± 81.62, n=8	660.7 ± 56, n=7
Perirhinal Cortex	334.7 ± 78.12, n=8	394.9 ± 47.22, n=8
Claustrum	605.5 ± 45.34, n=8	722.7 ± 69.23, n=8
Hippocampus (CA3)	17.35 ± 4.1, n=8	23.47 ± 3.085, n=8
Hippocampus (CA1)	14.54 ± 3.437, n=8	19.39 ± 3.876, n=8
Hippocampus (Dentate Gyrus)	73.98 ± 3.734, n=8	85.71 ± 10.09, n=8
Pedunculopontine Nucleus *	4.571 ± 1.043 n=7	8.125 ± 0.8332 n=8

* = p<0.05;

** =p<0.01